Interferometric Approaches to Evaluation of Strokes Camera and Object Rotation

2233005 Akter Monia
Principal Supervisor: Prof. Yoko Miyamoto
Supervisor: ：Prof. Eriko Watanabe

1. Introduction

There are two projects under the mentioned title. One is an interferometric method to evaluate the spatial resolution of Stokes camera using polarization fringes with different spatial frequencies. Another is an interferometric method for measuring the angle of rotation in the object plane in terms of the shift of the spectral peak.

2. Theory

2.1 Stokes Parameters and Stokes Camera

The Stokes parameter is a quantity that expresses the polarization state of light. The Stokes parameters are a set of values that describe the polarization state of an electromagnetic oscillation.

$$S_0 = I_{Vertical} + I_{Horizontal}$$

$$= I_{Right\ Diagonal} + I_{Left\ Diagonal}$$

$$= I_{Right\ Circular} + I_{Left\ Circular};$$

$$S_1 = I_{Horizontal} - I_{Vertical};$$

$$S_2 = I_{Right\ Diagonal} - I_{Left\ Diagonal};$$

$$S_3 = I_{Right\ Circular} - I_{Left\ Circular} \quad (2.1.1)$$

Stokes camera measures the polarization states of an optical field as a function of position by combining intensity distributions recorded under different polarization analyzer settings. It is not always easy to change the polarization analyzer settings without introducing spatial shifts, limiting the spatial resolution of such measurements. A dedicated Stokes camera can remove the necessity for external analyzers. But Stokes cameras are not necessarily designed to record polarizations states that vary rapidly in space. In this work we evaluate a Stokes camera in terms of how well it can record the polarization state that is changing rapidly in space.

2.2 Principle of Stokes Camera

In Figure 2.1 we show a possible hardware set up for a Stokes camera with an array of polarization filters. Only the intensity of a certain polarization component among the horizontally, vertically, right diagonally (45°) and right circularly polarized components can pass through the filter.

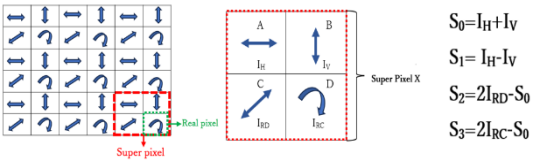

Figure 2.1: Polarization filter array and virtual super pixel made of real pixels of Stokes camera.

If we consider a virtual super pixel made of four real pixels, then the number of virtual super pixels will be one-fourth of the total number of real pixels of the camera. Each virtual super pixel can measure all the four polarization components in its four real

pixels to calculate the S_0 to S_3 Stokes parameters using equations (2.1.1).

3. Performance evaluation of Stokes camera

In this work we report an interferometric method to evaluate the spatial resolution of Stokes cameras. The method is applied to the evaluation of a Photonic Lattice WPI200 camera. The interferometer is used to create variations of polarization states with different spatial frequencies, and contrast in recorded Stokes parameters is measured.

3.1 Experiment

The experimental setup is shown in Fig. 3.1(a). A HeNe laser beam is expanded and collimated. The beam passes through either a polarizer (to create a diagonally polarized beam) or a quarter wave plate (to create a circularly polarized beam), then enters an interferometer. Due to the number of reflections the beams passing through the two arms of the interferometer become orthogonally polarized and create fringes in Stokes parameters S_1 and S_3 (interference between diagonally polarized beams), or S_1 and S_2 (interference between circularly polarized beams), which is recorded by the Stokes camera. Fringe spacings can be changed by adjusting Mirrors-1&2. The Stokes camera used in the experiment is controlled by the dedicated software WPI-Viewer. The recorded spatial distribution of S_1 is shown in Figs. 3.1(b) and 3.1(c).

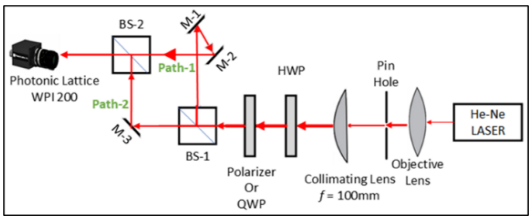

(a)

HWP = Half Wave Plate, QWP = Quarter Wave Plate, BS = Beam Splitter, M = Mirror

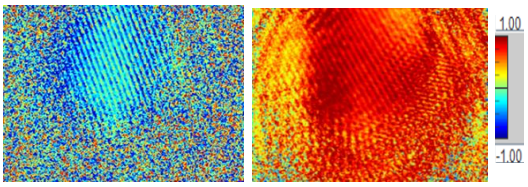

(b) (c)

Figure 3.1: (a)Interferometer (b) Interference between diagonally polarized light beams (c) Interference between circularly polarized light beams.

4. Data analysis

The fringes are analyzed for signs of degradation of contrast as the spatial frequency increases.

4.1 Calculation of Spatial Frequency

Figure 4.1(a) is a schematic diagram of the interference fringe. When the spatial frequency is 1/L, L corresponds to the interval between the peaks of the interference fringe.

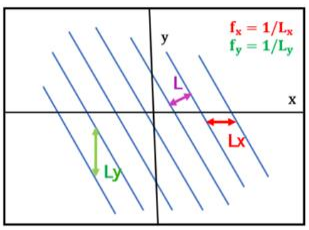

(a)

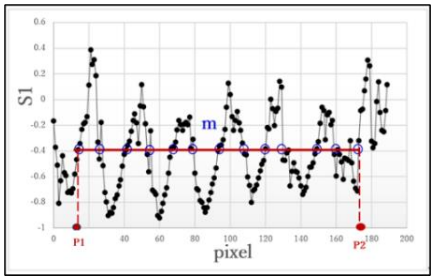

(b)

Figure 4.1: Theoretical model of calculating line spacing (L) and spatial frequency (f) from the recorded fringe pattern(a) and cross-section of the S_1 Stokes parameter spatial distribution (b).

Cross-sections of the interference fringes can be obtained in the x- and y-directions, respectively, and there are different spatial frequencies for each. The spatial frequency in the x-direction is $1/L_x = f_x$, and that in the y-direction is $1/L_y = f_y$. Fringe spacing L can be calculated by using equation (4.1.1) and spatial frequency f can be calculated from the fringe spacing L.

$$L = 1/\sqrt{\left(\frac{1}{L_x}\right)^2 + \left(\frac{1}{L_y}\right)^2} \qquad (4.1.1)$$

and $f=\frac{1}{L}$ (4.1.2)

A cross-section of the S_1 Stokes parameter spatial distribution is shown in figure 4.1(b). The cross-section in figure 4.1(b) has been compared with a sinusoidal wave with noise. P1 and P2 are two points marking the ends of a range of stable oscillations. Stable oscillation is an oscillation which has a relatively constant average and a relatively constant amplitude.

4.2 Calculation of contrast

In this study, the visibility is calculated as a measure of contrast. The amplitude is calculated from the cross-section of interference fringes as shown in figure 4.2. Since the data points contain noise, the visibility has been calculated by comparing the data with an ideal sine wave instead of using the data points directly. Contrast has been calculated as a ratio of S_1 change and average S_1. S_1 change has been denoted as X' in equation and (average S_1)+1 has been denoted as Y'. Contrast C is the ratio of X' and Y' and can written as equation (4.2.1).

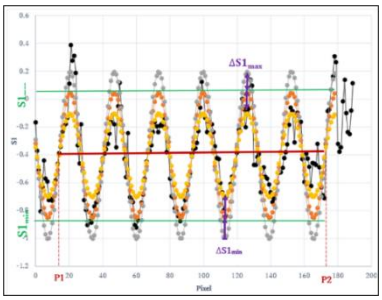

Figure 4.2: Comparison with ideal sine wave.

$$C = \frac{X'}{Y'} = \frac{\frac{S1max+1-S1min+1}{2}}{\frac{S1max+1+S1min+1}{2}} \qquad (4.2.1)$$

$$\Delta C = |C|\sqrt{\left(\frac{1}{X'}\right)^2 + \left(\frac{1}{Y'}\right)^2}\,\Delta =$$

$$|C|\sqrt{\left(\frac{1}{\frac{S1max+1-S1min+1}{2}}\right)^2 + \left(\frac{1}{Y\frac{S1max+1+S1min+1}{2}}\right)^2}\,\Delta \qquad (4.2.2)$$

The range of C which is ΔC has been calculated for all records. In this case, Δ is defined as follows

$$\Delta = \frac{\sqrt{\left(\Delta S_{max}\right)^2 + \left(\Delta S_{min}\right)^2}}{2} \qquad (4.2.3)$$

5. Assessing Contrast with Spatial Frequencies

Contrast vs. spatial frequency for diagonally polarized interfering light beams is shown in figures 5.1(a)and 5.1(b).

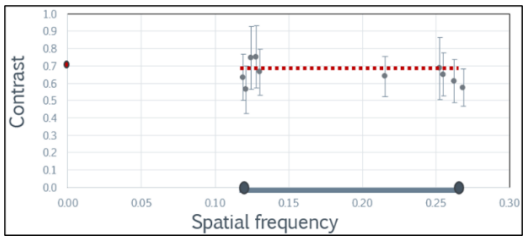

(a)

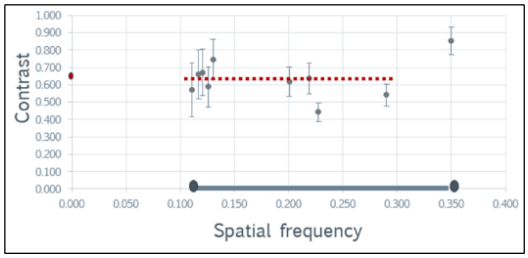

(b)

Figure 5.1 Contrast vs. spatial frequency for (a) S_1 and (b)S_3 for interference between diagonally polarized beams.

Contrast vs. spatial frequency for circularly polarized interfering light beams has been shown in figures 5.2(a) and 5.2(b).

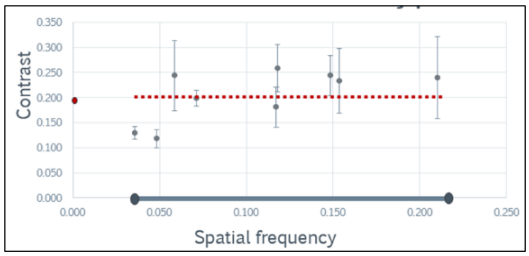

(a)

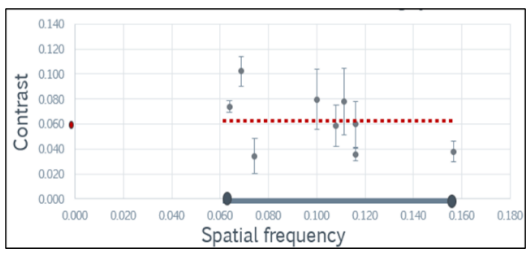

(b)

Figure-5.2: Contrast vs. spatial frequency for (a) S_1 and (b)S_2 for interference between circularly polarized beams.

6. Result:

For interference between diagonally polarized beams, contrast for Stokes parameter S_1 (fig 5.1a) is independent of spatial frequency in the range 0.12 to 0.27 pixel^{-1} . For S_3 in figure 5.1(b), contrast is independent of spatial frequency in the range 0.11 to 0.35 pixel^{-1}. For interference between circularly polarized beams, contrast for Stokes parameter S_1 in figure 5.2(a) is independent of spatial frequency in the range 0.06 to 0.157 pixel^{-1}. For S_2 in figure 5.2(b), contrast is independent of spatial frequency in the range 0.04 to 0.22 pixel^{-1}. Contrast is low for interference between circularly polarized light beams.

7. Measurement of In-plane Object Rotation

Previously, Lu et al. proposed and demonstrated a technique based on measuring rotation in terms of spatial distribution of horizontal movement [1]. The group extracted this movement as phase difference. They calculated the phase gradient from two points that were close together on the object surface to avoid phase unwrapping, limiting the accuracy of the measurement. Later Yang improved the technique by examining the spatial frequency spectrum in a similar interferometer, where the rotation angle has determined from the shift of the spectral peak [2]. However, the detection of the peak was done manually with limited resolution. In this work I have replicated Yang's results with a more compact interferometer.

7.1 Theory

The general expression for the phase change distribution $\Delta\varphi(x,y,z)$ is proportional to the projection of the displacement vector $\vec{l}$ (x, y, z) onto the sensitivity vector $\vec{k}(\vec{u},\vec{v},\vec{w})$.

$$\Delta\varphi(x,y,z)=\vec{k}(\vec{u},\vec{v},\vec{w}) \cdot \vec{l}(x,y,z) \quad (7.1)$$

l_x,l_y, and l_z are the x, y, and z components of the displacement vector. $\vec{u}$, $\vec{v}$ and $\vec{w}$ denote the unit vectors along the x, y, and z axis. The phase change caused by the object's arbitrary rotation can be determined by

$$\Delta\varphi(x,y,z) = \varphi_{after} - \varphi_{before} = \left(\overrightarrow{k_1} - \overrightarrow{k_{21}}\right)\vec{l}(x,y,z) - \left(\overrightarrow{k_1} - \overrightarrow{k_{22}}\right)\vec{l}(x+\Delta x,y,z) \quad (7.2)$$

λ is the wavelength of laser, $\overrightarrow{k_1}$ denotes the wave vector of the incidence beam, while $\overrightarrow{k_{21}}$ and $\overrightarrow{k_{22}}$ are the wave vectors of two object beams; α and β are the incidence angles.

$$\overrightarrow{k_1} = -\frac{2\pi}{\lambda}(\vec{w}) \quad ; \quad \overrightarrow{k_{21}} = \frac{2\pi}{\lambda}(\vec{u}\sin\alpha + \vec{w}\cos\alpha) \quad \& \quad \overrightarrow{k_{22}} = \frac{2\pi}{\lambda}(-\vec{u}\sin\beta + \vec{w}\cos\beta) \quad (7.3)$$

We consider that $\theta = \alpha = \beta$. Then equation (7.2) can be written as

$$\Delta\varphi(x,y) = -\frac{2\pi}{\lambda}[2\sin\theta \cdot l_x + \sin\theta \cdot \frac{\partial l_x}{\partial x} \cdot \Delta x] \quad (7.4)$$

Ω is the rotation angle of the object and l_x is the displacement in x direction,

$$l_x = x' - x = x\cos\Omega\text{-}y\sin\Omega\text{-}x$$

Partial derivative of l_x with respect to y and x are $\frac{\partial l_x}{\partial y} = -\sin\Omega$ and $\frac{\partial l_x}{\partial x} = \cos\Omega - 1$, respectively.

By putting the formula for $\frac{\partial l_x}{\partial x}$ in equation (7.4), we can show that

$$\Omega = \arcsin\left[\frac{\lambda}{4\pi\sin\theta} \cdot \frac{\partial(\Delta\varphi)}{\partial y}\right] \quad (7.5)$$

In the above equation $\frac{\lambda}{4\pi\,\mathrm{Sin}\theta}$ is a real number that will be determined by the interferometer.

7.2 Experiment

A He-Ne laser of wavelength 632.8nm is expanded. The collimating lens (f=100mm) lens is intentionally kept near the spatial filter (35mm) to get a larger beam area on the test object. The test object is an aluminum plate with rough surface.

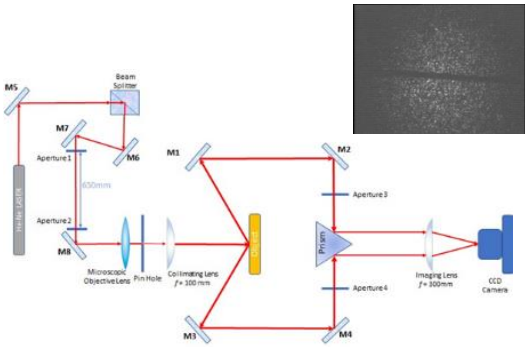

Figure-7.4: Optical setup and recorded interferogram (top right).

To make the imaging a little easier, a metal wire is pasted on the test object at the center of the beam. The incident beam gets scattered after hitting the test object. Two scattered beams are selected by apertures (diameter of 1mm). The two beams are then reflected by a prism towards the imaging lens and are observed on the image sensor of the CCD camera. Interferograms are obtained as the object is rotated in steps of 0.01°by using a rotation stage.

7.1 Fourier transform approach of In-plane object rotation.

The intensity of the interferometric speckle pattern before and after rotation of the test

object can be written as equation 7.1.1 and equation 7.1.2:

$$I_{before}(x,y) = a(x,y) + c_{before}(x,y)e^{i2\pi(f_{0x}x)} + c^{*}_{before}(x,y)e^{-i2\pi(f_{0x}x)} \quad (7.1.1)$$

$$I_{after}(x,y)=a(x,y) + c_{after}(x,y)e^{2\pi i (f_{0x}x)} + c^{*}_{after}(x,y)e^{-2\pi i(f_{0x}x)}. \quad (7.1.2)$$

We apply Fourier transform to the above equations (7.1.1) and (7.1.2) and denote as $I_{before\ FT}$ and $I_{after\ FT}$ respectively. They are given by

$$I_{before\ FT}(f_x, f_y) = A(f_x, f_y) + C_{before}(f_x - f_{0x}, f_y) + C^{*}_{before}(-f_x - f_{0x}, -f_y) \quad (7.1.3)$$

$$I_{after\ FT}(f_x, f_y)=A(f_x,f_y)+C_{after}(f_x - f_{0x}, f_y)+C^{*}_{after}(-f_x - f_{0x}, -f_y). \quad (7.1.4)$$

$c_{before}(x,y)$ and $c_{after}(x,y)$ can be reconstructed by filtering, shifting, and applying inverse transform to C_{before} and C_{after}.

We define

$$d(x, y) = c_{before}(x,y)\, c^{*}_{after}(x, y) \quad (7.1.5)$$

and its Fourier transform

$$F[d(x,y)] = D(f_x, f_y). \quad (7.1.6)$$

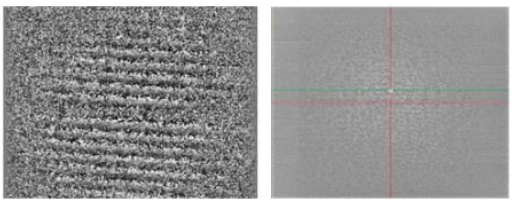

(a) (b)

Figure-7.5: (a) Phase distribution of $c_{before}(0.00°) \times c^{*}_{after}(0.03°)$ (b) Fourier transform of (a)

For small rotation we can show that $c_{after}(x,y) \sim c_{before}(x,y)e^{-2\pi i f_s \Omega y}$, so that

$$d(x, y) = d_{\Omega=0}(x, y)e^{2\pi i f_s \Omega y}, \quad (7.1.7)$$

$$D(f_x, f_y) = D_{\Omega=0}(f_x, f_y - f_s\Omega) \quad (7.1.8)$$

$f_s\Omega$ is the amount of shift of spectral peak in f_y direction and has been observed as shown in figure-7.5.

7.6 Result

With the increase of the rotation angle, it has been observed that the spectral peak shifts in the y direction as in Yang's work. The rotation angle is expected to be proportional to the amount of shift of the spectral peak. Compared to Lu's method, this technique is expected to have less error because it uses information from the entire image instead of two close points.

Summary

In this paper, the performance evaluation of the spatial resolution of the WPI-200 Stokes camera has been done. Polarization fringes of different spatial frequencies have been recorded. Spatial resolution has been found to be independent of the spatial frequency.

A compact optical system has been realized for the measurement of in-plane object rotation angle. The interferograms have been recorded and partially processed according to the proposed method, and the shift in frequency space has been observed.

References

[1] Min Lu et al., Opt. Lett. **42**, 1986 (2017).

[2] YANG ANDONG 「空間周波数成分に注目した面内回転角測定の実験的検証」, 電気通信大学 修士論文, (2022)